PACS 81.05.Dz, 81.15.Cd

The influence of physical and technological magnetron sputtering modes on the structure and optical properties of CdS and CdTe films

G.S. Khrypunov, G.I. Kopach, M.M. Harchenko, A.I. Dobrozhan
National Technical University "Kharkiv Polytechnic Institute"
21, Kirpichov str., 61002 Kharkiv, Ukraine
E-mail: gkopach@ukr.net

Abstract. To create technology for preparation of CdS and CdTe thin films by direct current magnetron sputtering, the influence of physical and technological condensation modes on the crystal structure and optical properties of these films were investigated. The laboratory method of DC magnetron sputtering with preheating of the target for the mentioned films on glass substrates was developed. We obtained the CdS layers with hexagonal structure 150…200 nm thick under conditions when the plasma discharge current density was 1.1 mA/cm^2 and the deposition rate – 30…40 nm/min. The bandgap in the obtained CdS films is E_g = 2.38…2.41 eV. After annealing in vacuum, the optical transparence of CdS films reaches 80…90%, which allows to use these films as a transparent window layer in solar cells based on heterojunctions of CdS/CdTe. When the plasma discharge current density is 2.2…5.4 mA/cm^2 and the deposition rate is 200 nm/min, we obtained CdTe layers with hexagonal structure up to 5 μm thick. The transmittance of CdTe films with hexagonal structure in the wavelength range of the visible spectrum is up to 5%, and in the infrared spectral range is about 60%. The bandgap in the obtained CdTe layers of different thickness is 1.52…1.54 eV. After chloride treatment as a result of the phase transition wurtzite–sphalerite, the investigated CdTe films contain only the stable cubic structure and can be used as a base layer of solar cells.

Keywords: cadmium telluride, cadmium sulfide, direct current magnetron sputtering, thin films.

1. Introduction

Thin-film solar cells based on cadmium sulfide (CdS)/cadmium telluride (CdTe) heterojunction are prospective for industrial production [1-3]. In heterosystems *n*-CdS/*p*-CdTe, the CdS layer is used as the window one. It allows to reduce a negative impact of surface recombination of non-equilibrium charge carriers by removing their active generation area from the illuminated surface. One of the economical and high-tech methods for thin films is magnetron sputtering [4]. Implementation of the radio-frequency magnetron sputtering regime for CdS and CdTe films allows to

prevent accumulation of the excess electric charge on the surface of the target. But this method is expensive, energy intensive and requires a special technological equipment. Ukrainian electronic industry mastered the high-tech and economical method of direct current magnetron sputtering (DC magnetron sputtering) of materials. However, there are some technological problems during deposition of semiconductor films by this method. They are caused by low conductivity of CdS and CdTe pressed powder targets and sufficiently low emission ability of these materials. Therefore, the development of DC magnetron sputtering of semiconductors and the study of crystal structure and optical properties of CdS and CdTe films grown under

different physical and technological modes of condensation are relevant.

2. Experiments

In laboratory technology for condensation of CdS and CdTe films by using DC magnetron sputtering, it was used the design of VUP-5m magnetron, which feature was that the cooling circuit covered only the magnetic system with the result that there was no forced cooling of the sputtered semiconductor pressed powder target. To implement the process of thermionic emission of electrons from the target material for plasma discharge ignition, the target was preheated for 10…15 min.

CdS films were condensed on soda-lime glass substrates at different physical and technological modes: substrate temperature T_{sub} = 120…200 °C, pressure of inert gas P_{Ar} = 0.9…1 Pa, magnetron discharge current density J = 1.1 mA/cm^2, the voltage on magnetron V = 550…600 V, deposition time 5 min. When manufacturing CdS/CdTe based solar cells, the base CdTe layer is condensed on CdS layer at T_{sub} > 300 °C. The effect of annealing in vacuum 10^{-4} Pa at 400…420 °C for 30 min on the structure and optical properties of CdS layers was investigated.

CdTe layers were also obtained on soda-lime glass substrates under the following conditions: T_{sub} = 295…315 °C, P_{Ar} = 0.8…1 Pa, J = 2.2…5.6 mA/cm^2, V = 600…650 V, deposition time 15…25 min. To determine the effect of heat treatment on the structure of CdTe samples, the CdTe layers annealing was carried out in vacuum at T = 400 °C for 20 min.

To use the obtained CdTe films as base layers of solar cells, there was performed chloride treatment (Cl treatment) in vacuum P = 5.3·10^{-3} Pa and temperature of CdCl$_2$ evaporator 470…475 °C for 5 min with subsequent annealing in air at T = 430 °C for 25 min [5].

The structure of the obtained CdTe and cadmium sulfide films was studied using the X-ray diffractometry (XRD) methods [6]. There was performed automatic recording of X-ray spectra at θ-2θ scanning by using X-ray diffractometer DRON-4 with the step 0.01…0.02 degrees in K$_α$-radiation of cobalt anode.

To accurately determine the phase composition of the obtained CdTe films, we used the "oblique" shooting method, during which in the radiation of cobalt anode in the process of θ-2θ scanning performed were detection and registration of diffraction reflections from those sphalerite and wurtzite planes that are not detected in the foregoing registration method because of texturing of samples.

The CdTe cubic structure lattice parameter was determined using the formula:

$$a = d\sqrt{h^2 + k^2 + l^2} \ , \qquad (1)$$

where d is the interplanar spacing.

For precise determination of the lattice parameter, the Nelson–Rhyl extrapolation method was used.

Optical studies of CdTe and CdS layers were carried out using the spectrometer SF-2000. The transmission spectrum of studied films was used to determine the thickness of the layers according to [7]. The thickness of the layers was determined using the formula:

$$t = \frac{M \cdot \lambda_1 \cdot \lambda_2}{2\left(n(\lambda_1) \cdot \lambda_2 - n(\lambda_2) \cdot \lambda_1\right)} \ , \qquad (2)$$

where λ_1, λ_2 are the wavelengths of two adjacent extremums (interferential maxima or minima of transmission spectrum) in nm; $n(\lambda_1)$, $n(\lambda_2)$ – refractive index, depending on the wavelengths λ_1, λ_2.

The bandgap of thin films was determined by calculating the dependence of absorption coefficient on the wavelength α(λ) using [8]:

$$T = (1 - R) \cdot e^{-\alpha \cdot t} \ , \qquad (3)$$

where T is the transmission coefficient; R – reflection coefficient; t – film thickness.

The bandgaps of CdTe and CdS polycrystalline films were determined by extrapolation of the linear portion of the $(\alpha \cdot h\nu)^2 = f(h\nu)$ curves (where h – Planck constant, ν – frequency) to the intersection with the $h\nu$ energy axis.

3. Results and discussion

When studying the XRD patterns of the lattice of CdS layers grown at different substrate temperatures T_{sub} = 120…200 °C (Fig. 1), the only one diffraction peak was observed for all of the received films at the angle 2θ = 30.62°. This peak corresponds to reflection (111) of cubic structure or (002) hexagonal phase of CdS. A low intensity of this peak is caused by a small thickness of the sample. It does not allow to accurately determine the phase composition of the CdS samples using the XRD methods.

But considering that the CdS stable structure is hexagonal [9], subsequent diffractogram data processing (Table 1) was done for this CdS phase. For all the samples, the intensity of peak lies in the 220-280 imp/s range, which indicates almost the same thickness of obtained CdS layers. The estimated values of interplanar spacing lie in the 3.379…3.391 Å range, which corresponds to the value of lattice parameter c = 6.758…6.782 Å. The obtained values of the parameter c are bigger than the table value for single crystals (c = 6.7198 Å, PCPDFWIN# 411049) and indicate the presence of macrostresses. The full width at half maximum (FWHM) of the peaks in the 0.3…0.38 degree range on the 2θ scale are typical for CdS thin layers obtained using vacuum methods [10] and caused by small grain sizes of the film.
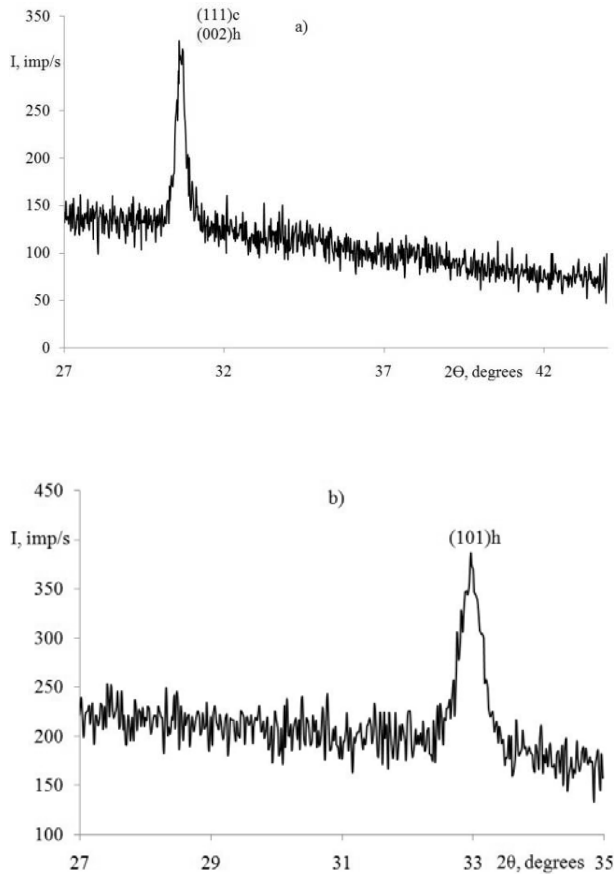
Spectral dependences of transmission coefficient for the obtained CdS layers are presented in Fig. 2. According to results of optical studies there is a strong absorption of radiation in the wavelength range 400 to 500 nm, while in the infrared spectral range the CdS films transparence is up to 80%. The typical thickness of investigated CdS layers is 150…200 nm. The bandgap in the prepared CdS films is E_g =2.38…2.41 eV, which is close (E_g = 2.42…2.45 eV) to that of CdS single crystals.

After annealing of CdS layers in vacuum, in the XRD pattern (Fig. 1b) only one intense peak was detected at the angle $2\theta = 32.8°$, which corresponds to reflection (101) of stable CdS hexagonal phase. The optical transparence of CdS films is up to 90% over the entire spectral range, which indicates the ability to use these films as a transparent window layer in solar cells based on heterostructure of CdS/CdTe [10].

We investigated the structure and optical properties of CdTe thin films grown on glass substrates using DC magnetron sputtering method at different physical and technological condensation modes (Table 2).

The typical XRD patterns of CdTe sample layers obtained at different physical and technological condensation modes (samples 3, 4, 6, 7) are shown in Fig. 3 (by the example of sample 6).

In all diffractograms of the studied CdTe films, there are two distinct peaks at the angles 2θ 27.05° and 91.05°. According to the table ASTM 15-0770, they can belong both to hexagonal and cubic structures of CdTe: wurtzite reflections (002) and (006) and sphalerite reflections (111) and (333), respectively. Also, the reflections (103) and (105) of hexagonal phase CdTe are observed in diffractograms.

Fig. 1. XRD patterns of the obtained CdS sample layer (a) and after its annealing (b).

Table 1. CdS films diffractograms processing results.

Sample №	T_{sub}, °C	Peak position, degrees	Interplanar spacing, Å	Intensity, imp/s	FWHM, degrees
2	120	30.62	3.388	216	0.33
3	130	30.59	3.391	280	0.33
1	150	30.58	3.391	44	0.38
4	175	30.63	3.386	260	0.30
6	180	30.64	3.385	269	0.34
5	200	30.70	3.379	234	0.30

Table 2. Technological modes of obtaining CdTe films.

№	T_{sub} at start, C	T_{sub} at finish, C	t, min	P_{Ar}, Pa	U, V	I, mA
1	330	315	15	0.8–1	600	60
2	300	300	15	0.8–1	600	40
3	295	292	25	0.8–1	600	40
4	300	300	25	0.8–1	600	60
5	270	315	15	0.9–1	600	80
6	312	295	25	0.9–1	650	80
7	312	297	15	0.8–0.9	650	100
8	300	316	25	0.9–1	600	80
9	300	313	25	0.9–1	600	80
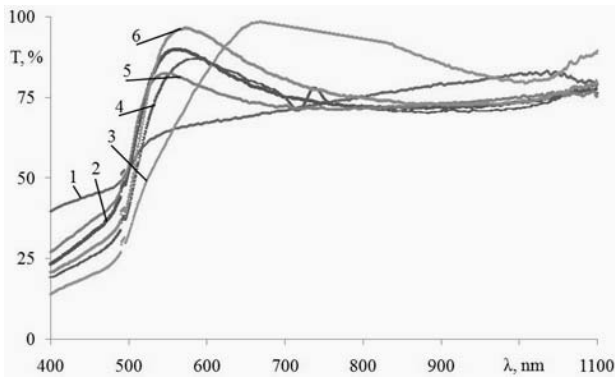
**Fig. 2.** Spectral dependences of the transmission coefficient for the samples 1 to 6, respectively.
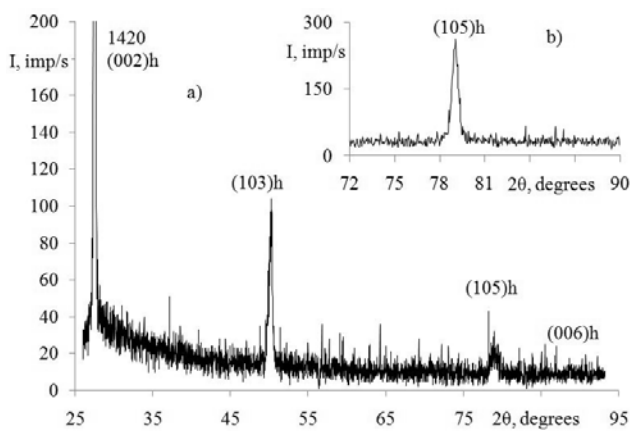
Fig. 3. Typical XRD patterns of the obtained CdTe films: (a) sample 6, (b) sample 6, by using the "oblique" shooting method.

Using the "oblique" shooting method of diffractometry at the angles 2θ 72° to 85° allowed determining the exact phase composition of grown CdTe layers when rotating the sample by the angle 20.5°. In all diffractograms, only the reflection (105) of hexagonal phase was observed (Fig. 3b). Thus, all the studied CdTe films obtained in different physical and technological condensation modes by DC magnetron sputtering method contain only metastable hexagonal structure. The annealing of samples in vacuum at $T = 400\,°C$ for 20 min does not change the CdTe layers phase.

Traditional Cl treatment of the studied CdTe films facilitates phase transition wurtzite–sphalerite, what can be seen in XRD patterns. The typical diffractogram of the sample 8 (Table 2) is shown in Figs. 4a and 4b.

All peaks that belong to the stable cubic structure CdTe are observed. Using the "oblique" shooting method at the angles 2θ 72.5…87.5°, when rotating the sample by the angle 20.5°, it was found that, in this area of XRD pattern, only cubic structure peaks (331) and (422) can be observed, hexagonal structure peaks (105) are not presented. Thus, Cl treatment facilitates phase transition wurtzite–sphalerite, thereby studied CdTe films contain only stable cubic structure.
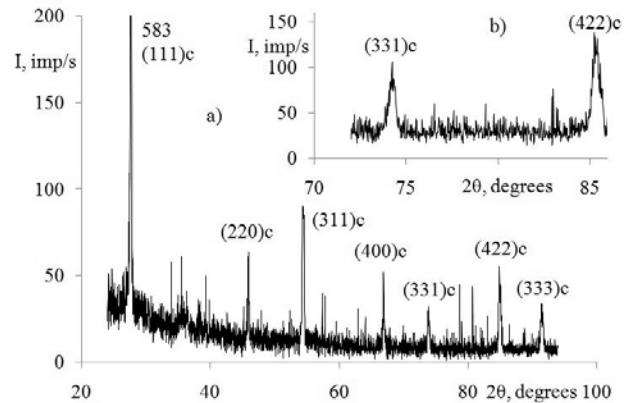

Fig. 4. XRD pattern of the sample 8: (a) after Cl treatment and annealing in air and (b) by using the "oblique" shooting method.

After Cl treatment, we observed a slight decrease of FWHM values of peaks (111) and (333) as compared with the peaks (002) and (006) of hexagonal phase in the samples before Cl treatment and annealing in air (Figs. 1 and 4). This indicates the passing of the recrystallization process and grain size increasing in the polycrystalline CdTe films. The calculated value of lattice parameter in the cubic structure of CdTe films after Cl treatment is $a = 6.4905$ Å. The deviation from the value a in the table ASTM 15-0770 is less than 0.2%.

Spectral dependences of the transmission coefficient for CdTe film samples 1-9 are shown in Fig. 5 (Table 2).

For all the samples, there is a strong absorption of radiation within the wavelength range 400…700 nm and sharp fall at the band edge within the range 750…800 nm. In the infrared spectral range, the transparence of films 4 and 5 is about 65%, films 2 and 3 is about 50%, films 1, 6, 8 and 9 is about 30%.
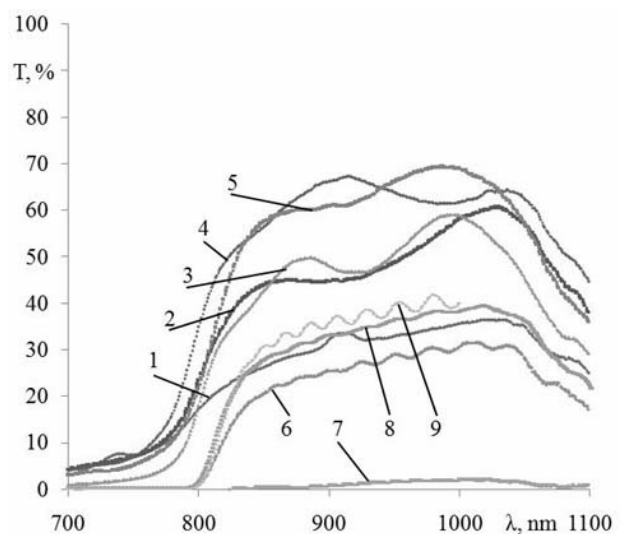
Fig. 5. Spectral dependences of the transmission coefficient for the samples 1 to 9.

Table 3. The value of the bandgap for CdTe films of different thicknesses.

№	t, min	I, mA	T, C	Film thickness, nm	E_g, eV
1	15	60	315	300	1.51
2	15	40	300	390	1.53
3	25	40	292	1030	1.51
4	25	60	300	2360	1.5
5	15	80	315	2120	1.52
6	25	80	300	5200	1.52
7	15	100	297	5500	–
8	25	80	316	4900	1.54
9	25	80	312	5000	1.53

The obtained results for the film thickness and bandgap based on optical researches are presented in Table 3.

Being based on the calculated values of the CdTe film thickness that differs by the condensation time, the condensation rate that depends on the plasma discharge current was calculated (Fig. 6).

The average deposition rate of CdTe films increases with increasing the plasma discharge current regardless of the condensation time. Increasing the slope of the plot areas at a discharge current higher than 60 mA indicates that the chosen magnetron operation mode provides sufficiently high increasing the film deposition rate. The fact, that when the condensation time is 25 min, the average deposition rate of film is higher than in the case $t = 15$ min, is caused by the simultaneous occurrence of two processes: target sputtering and increasing its material sublimation rate with an increase of its temperature due to Ar ions bombing. When the plasma discharge current was >80 mA, it was got the high enough rate of condensation reaching the level 150…200 nm/min. At identical operating parameters of the magnetron and Ar pressure in vacuum chambers, the relative difference of CdTe films thickness is lower than 2% (Table 1, samples 6, 8 and 9).
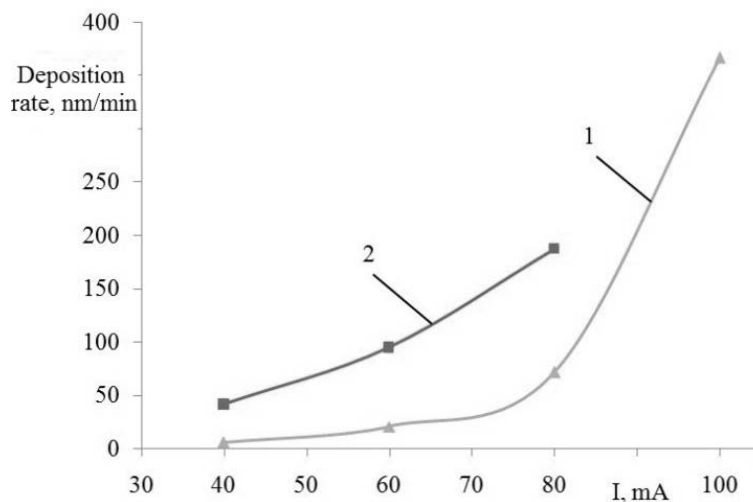
Fig. 6. Dependence of the average CdTe film deposition rate on the discharge current in the mentioned modes for condensation time 15 (*1*) and 25 (*2*) minutes.

4. Conclusions

The laboratory method of DC magnetron sputtering with preheating of the target for CdS and CdTe films on soda-lime glass substrates was developed. The CdS layers with hexagonal modification 150…200 nm thick under conditions when the plasma discharge current density is 1.1 mA/cm^2. The deposition rate 30…40 nm/min was obtained. The bandgap in these CdS films is $E_g =$ 2.38…2.41 eV. After annealing in vacuum, the optical transparence of CdS films is 80…90%, which allows to use these films as a transparent window layer in solar cells based on the heterostructure CdS/CdTe.

When the plasma discharge current density is 2.2…5.4 mA/cm^2 and the deposition rate is 200 nm/min, CdTe layers with hexagonal structure up to 5 μm thick were obtained. The transmittance of CdTe films with the hexagonal structure in the wavelength range of the visible spectrum is up to 5%, and in the infrared spectral range is about 60%. The bandgap in the obtained CdTe layers of different thickness is 1.52…1.54 eV.

After Cl treatment with subsequent annealing in air at $T = 430$ C for 25 min, as a result of the phase transition wurtzite–sphalerite, the investigated CdTe films contain only the stable cubic structure, which value of the lattice parameter is $a = 6.4905$ Å, which by less than 0.2% deviates from the tabular value. These CdTe films can be used as a base layer of CdS/CdTe based solar cells.

References

1. Bosio A., Romeo N., Mazzamuto S., Canevari V. Polycrystalline CdTe thin films for photovoltaic applications. *Prog. Cryst. Growth Charact. Mater.* 2006. **52**, No. 4. P. 247–279.

2. Hädrich M., Heisler C., Reislöhner U., Kraft C., Metzner H. Back contact formation in thin cadmium telluride solar cells. *Thin Solid Films.* 2011. **519**, No. 21. P. 7156–7159.

3. Wu X. High-efficiency polycrystalline CdTe thin-film solar cells. *Solar Energy.* 2004. **96**. P. 803–814.

4. Li H., Liu X. Improved performance of CdTe solar cells with CdS treatment. *Solar Energy.* 2015. **115**. P. 603–612.

5. Kharchenko N.M., Khripunov G.S., Li T.A. Technology optimization of the chloride treatment of cadmium chalcogenide thin films. *JPSE.* 2008. **6**, No. 3-4. P. 128–133.

6. Panchekha P.A., Alaverdova O.G., Gnidash V.I. Heterophase state and polytexture of CdTe films deposited from the ion-molecular beam. *Ukr. J. Phys.* 2000. **45**, No. 1. P. 75–80.

7. Brus V.V., Solovan M.N., Maystruk E.V. et al. Specific features of the optical and electrical properties of polycrystalline CdTe films grown by the thermal evaporation method. *Physics of the Solid State.* 2014. **56**, No. 10. P. 1947–1951.

8. Salem A.M., El-Ghazzawi M.E. Structural and optical properties of chemically deposited CdCr$_2$S$_4$ thin films. *Semicond. Sci. Technol.* 2004. **19**. P. 236–241.

9. Aven M. and Prener J.S. *Physics and Chemistry of II-VI Compounds.* North-Holland & John Wiley and Sons, Amsterdam & New York, 1967.

10. Khrypunov G., Romeo A., Kurtzesau F., Batzner D.L., Zoggand H., Tiwari A.N. Recent developments in evaporated CdTe solar cells. *Solar Energy Materials & Solar Cells.* 2006. **90**, No. 6. P. 664–677.